International Journal of Refrigeration 178 (2025) 160–169

Contents lists available at ScienceDirect

International Journal of Refrigeration

journal homepage: www.elsevier.com/locate/ijrefrig

INSTITUT INTERNATIONAL DU FROID
INTERNATIONAL INSTITUTE OF REFRIGERATION

Thermal design of an ejector-supported cycle using krypton for cooling of particle detector accelerators

Luca Contiero [a,b,*], Krzysztof Banasiak [b,c], Bart Verlaat [a], Armin Hafner [b], Sven Försterling [d], Yosr Allouche [b]

[a] European Organization for Nuclear Research, Geneva 1211, Switzerland
[b] Norwegian University of Science and Technology, Trondheim 7491, Norway
[c] SINTEF Energi AS, Trondheim 7034, Norway
[d] TLK-Thermo GmbH 38106, Braunschweig, Germany

ARTICLE INFO

Keywords:
Innovative ejector cycle
Detectors
Thermal shock
Krypton

ABSTRACT

According to the High-Luminosity plan (HL-LHC) the Large Hadron Collider will be upgraded to further extend physics discoveries (2033–2034). The increase of the luminosity is followed by an increase of the radiation damage on the silicon sensors used to detect those particles, which they must be preserved from the thermal runaway after which the sensors reach electrical breakdown. The future upgrade will require to the cooling system temperature levels ranging from -60 to -80 °C, currently unattainable by the CO_2 cooling technology (2PACL). From a previous study the noble gas krypton was selected for the thermal management of future detectors as working medium. To meet the requirements of the new generation of particle accelerators, a new ejector-supported cooling system was proposed.

In this work, thermal design of the innovative ejector cycle was carried out starting from the detector. The semi-passive detector loop was first designed to ensure optimal working conditions of the detector. Liquid krypton is supplied to the detector by the ejector, maintaining a constant pressure lift independently of the operating temperature, with a flow variation not exceeding 4.3 % of the design value. The boundary conditions expressed by pressure, density and flow rates will serve as inputs for the design of the adjustable geometry ejector. To verify the thermal stability along the detectors, development of a control strategy to handle setpoint changes and sudden change in the cooling power is also addressed. The off-design case with fluctuating heat loads shows an offset in the evaporating temperature below 0.3 K.

1. Introduction

The largest and most energetic accelerators worldwide called Large Hadron Collider (LHC) is located at CERN, the European Organization for Nuclear Research. The Large Hadron Collider is a super-conducting accelerator installed in a 27 km long circular tunnel that is buried 100 m underground. It is used to study the basic constituents of matter through the tracking of path and momentum of particles which are accelerated in two counter-circulating bunches before colliding in proximity of the so-called interaction point. At the collision point, new particles are created and spread in all the directions around the beam pipe. A powerful magnet installed around the interaction point provides a strong magnetic field that bends the trajectories of all the charged particles created in the collision to derive their momentum and charge. The extreme precise spatial reconstructions of tracks are obtained through a hermetic multi-shell closed volume. Coaxial cylinders, so-called “Barrels” are mounted around the beam pipe where the largest radiation dose is registered. Up to a certain distance from the beam pipe, the layers are organized as disks perpendicular to the beam (so-called “EndCaps”). Detector trackers normally comprise different type of semiconductor detector technologies. In the outer layers of the tracker, elongated semiconductor arrays arranged alongside each other called strip modules, allows to reconstruct the trajectories of particles. The electrical charges created by the particle crossing are recorded by the read-out electronics installed close to the modules. The pixel modules, consisting in sensing elements arranged in two-dimensional arrays, have the readout chips directly installed below the model. They are installed in the innermost layer providing a very precise spatial resolution and

* Corresponding author.
E-mail addresses: luca.contiero@cern.ch, luca.contiero@ntnu.no (L. Contiero).

https://doi.org/10.1016/j.ijrefrig.2025.06.030
Received 12 September 2024; Received in revised form 25 June 2025; Accepted 26 June 2025
Available online 26 June 2025

high signal-to-noise ratio (Seidel, 2019). Four larger experiments, characterized by different energy density, are located at CERN and they are known as ATLAS, CMS, LHCb and ALICE experiments. The radiation level in proximity of those detectors is an indication of the damage to the silicon sensors, which must be protected and preserved to maintain their functionality and efficiency (Beck and Viehhauser, 2010). With the launch of the physics program of the LHC (Pettersson and Lefèvre, 1995), a radical innovation of the conception of the tracker and associated cooling system began. The goal of the cooling system is to maintain the sensors cold and at a controlled temperature, maximizing the signal to noise ratio.

In the old generation of particle detectors, single-phase water cooling in a sub-atmospheric system was used as the radiation level was sufficiently low (ATLAS collaboration, 1997). However, with the advancement of the semiconductor technology and increase of the radiation dose, the high freezing point of water and being electrically conductive pushed the need for novel technologies. The initial approach of using water-based mixture with freezing point depressant fluid as methanol was dropped in favor of an evaporative cooling system using perfluorocarbons (C_3F_8) for cooling of the sensors down to −20 degree celsius, thanks to its dielectric properties, molecular stability and non-flammability (Anderssen and others, 1999; Attree et al., 2008). The first system was an oil-free compressor-based cooling cycle which suffered by fatigue problems on the compressors that caused frequent failures and leaks. In addition, a controlled cooldown of the sensors especially during critical transient as the startup was difficult to achieve, leading to an electric failure of many silicon modules and strongly reducing their lifetime due to the exposure to thermal shocks. As an alternative to the C_3F_8 compressor-based system, a gravity-driven C_3F_8 thermosiphon system was designed and launch in operation in 2015 (Battistin et al., 2015) while the compressor-based cycle became the backup unit. However, at low evaporating temperatures, the poor thermal performance of the fluid concerning the low operating pressure made a new evaporating cooling solution with CO_2 gaining popularity until it was chosen as cooling solution in the cosmic particle detector AMS-02 (Van Es et al., 2004; Zhang et al., 2011) and in the LHCb Velo detector (Verlaat et al., 2008). Afterwards also the ATLAS ITk (Inner Tracker), which is the innermost detector directly located around the interaction point where hardware minimization is even more demanding, adopted a CO_2 cooling-based solution. The diameter of the cooling channel with CO_2 could have been reduced by approximately a factor four, while maintaining an acceptable temperature difference between inlet-outlet of each evaporative cooling line. The temperature budget, defined by a maximum allowable temperature difference of 3 K between the inlet and outlet, serves as a key specification for selecting the optimal design.

According to the High Luminosity plan (HL-LHC), a major upgrade of the entire underground infrastructure will take place in 2033–2034 (ECFA Detector RandD Roadmap Process Group, 2020). Following periods of operation (Run), the LHC is stopped for one or more years during the so-called Long Shutdowns (LS) to carry out maintenance, consolidation, or a complete upgrade of each sub-detector. The next major upgrade (LS4) will see the detectors interested by unprecedent level of high particle densities. Today's cooling system operating with CO_2 has reached its temperature limitation due to the triple point location, i.e., −56 degC. The 2PACL (two-phase accumulator pumped loop) is part of a cascade refrigeration system aimed to remove the heat released by the sensors. At detector level, the minimum temperature attainable is around −40 °C, considering the subcooling required at the pump inlet and the increasing temperature losses of the fluid while operating at low operating pressures (Tropea et al., 2016; Zwalinski et al., 2023). As a result of such limitations, thermal runaway of the sensors is predicted for the future detector upgrade if no measures are taken.

For this reason, as part of a large study, a preliminary study on environmental-friendly refrigerants for operation at temperatures below −50 °C showed the noble gas krypton as potential candidate for thermal management of future detectors, with the possibility to go as low as its triple point (≈ −157 °C) (Contiero et al., 2024). A new ejector-supported system using krypton was developed (Contiero et al., 2024) with extensive functionality to cope with the harsh detector requirements. In this study, the thermal design of the system is addressed, and guidelines for the future system's design are discussed as this is crucial for the upcoming steps into the experimental verification of the cycle technology. Given the wide range of operating conditions covering both gas/-supercritical and two-phase states, the design of the system was based on the latter phase mentioned. Since the detectors are the most sensitive components, the design initially focuses on providing an architecture that meets their stringent requirements. The flow rates and the pressure levels obtained from the design of the detector cooling loop are essential to dimension the adjustable geometry ejector. As last, dynamic modelling and development of a control strategy aiming to provide a stable and controlled cooling were addressed.

2. Specific requirements of the detector cooling system

Silicon detector trackers are exposed to different temperature levels during their lifetime, starting from room temperature during the commissioning phase down to the cold temperatures required to run physics experiments. The gas state of krypton at room temperature poses challenges never experienced so far for detector cooling. Operation and design guidelines of gas/supercritical cycle is quite limited and only power system based on the Brayton cycle using supercritical CO_2 serve as reference (Moisseytsev et al., 2009). However, important insights can be drawn for the existing supercritical CO_2 cycles such as pressure regulation of the cycle and the dynamics concerning the single-phase state of the fluid (Mahapatra, 2018; Trinh, 2010). For such reasons the system designed was based on the two-phase area, where the detector operation is provided by flow boiling (below −70 °C). Conversely to the existing two-phase pumped loop approach (2PACL) (Verlaat, 2007), the use of a vapor compression system creates different challenges. Oil-free is mandatory due to break chain of the molecular structure of the lubricants in a high-irradiated environments. Oil-free compressors experiencing high densities difference at the suction (while moving from warm to cold temperatures) are hard to design and they normally require more maintenance than oil-lubricated compressors. As occurred with the old cooling system at CERN using C_3F_8 (Attree, 2008), to address the high level of reliability a redundant compressor pack is strongly recommended to take over the other compressor group during maintenance.

As a short summary of the key requirements presented in (Contiero et al., 2024), serving as basis for designing of the cooling system:

- For low-mass detector design it is extremely important to minimize the hardware installed close to the detector, reducing the perturbances to the measurements.
- Avoid thermal shocks while gradually cooldown the detectors, especially considering their limited thermal mass and inertia. Controlling the fluid temperature entering the detectors is of primary importance.
- For two-phase cooling it is imperative to work safely away from risk of dry-out. Vapor quality measurements, normally difficult to be performed, are discouraged by the lack of space and as rule of thumb a vapor quality limit of 35 % is normally considered.

The latter requirement introduces the challenge of delivering only vapor to the compressor suction port due to the incompressibility of the liquid phase. The two-phase state at the detector outlet demands different solutions at system level. The simplest and more inefficient solution is to use a heater to fully vaporize the exhaust two-phase flow (Attree, 2008). A more efficient way is the use of an ejector which acts as a pumping device regulating the flow through the detectors. Each of the

previous solutions influences the system architecture. Krypton properties and ejector working mode precludes to follow up the detector working conditions, requiring a compressor design to withstand a wide variation of temperature-pressure (densities). The cooling system developed at CERN using C_3F_8 was designed such to work with fixed conditions at the compressor suction. Cooling capacity was controlled via bypass regulation and the evaporating temperature with a back-pressure regulator, throttling the flow from the detector outlet down to the suction pressure of the compressors. This methodology was applicable because of the two-phase state of the fluid all over the operating range.

Passive expansion devices are required due to the unfeasibility of performing maintenance in a high-irradiated environment. In some detectors, capillaries are also used to cover the distance between manifolds and evaporators while at the same time promoting expansion of cold liquid into the two-phase zone characterized by low vapor content. The subcooled liquid at the capillary entrance is supplied by a tube-in-tube heat exchanger while further vaporizing the exhaust two-phase flow at the detector outlet. The concentric line must be designed to ensure the supply of the required subcooled state at the capillary entrance while having low pressure drops on both lines. The sum of the pressure drops across the different components represents the pressure lift that must be provided by the ejector. Maintaining a small pressure gradient on the return line provides a direct control of the outlet evaporating temperature.

3. Conceptual design of the ejector-supported system

The cycle architecture of the new cycle is presented in Fig. 1, for more details the reader is referred to (Contiero et al., 2024). The cooling system resembles a traditional vapor compression unit equipped with an ejector to drive liquid-gas recirculation through the detectors. The schematic here presented includes an additional valve in the detector loop ("bypass detectors"), which serves as additional protection for flow control especially during the cycle startup where thermal shock is an extreme concern.

The design followed in this study is a stepwise approach which combines performance of krypton cooling in mini-channels, ejector working principle and temperature requirements. The expected temperature range of interest lies between −60 to −80 °C. As broadly discussed in (Contiero et al., 2024), high-pressure fluids offer better performance than low-pressure fluids, accepting higher pressure drops while resulting in lower temperature gradients. Maintaining low temperature gradients among inlet-outlet preserves the integrity of the sensors, although the fluid heat transfer coefficient should not degrade excessively to preserve the same heat removal capability along the cooling line.

During flow boiling operation is important to maintain the liquid receiver in two-phase state: this has an influence on the pressure regulation methodology which differs between supercritical and transcritical operation. By having the liquid receiver in the two-phase state, the maximum allowable evaporating temperature decreases as a function of the pressure drops upstream the evaporator section. The range here considered is within −70 to −80 °C, corresponding to the reduced pressure between 0.62–0.84.

The estimation of the thermohydraulic performance in the evaporator section is the first step. Such conditions, in terms of flow rate, temperature and pressure, are supplied via the ejector and dependent on the design of the different components surrounding the detector volume (i.e. capillaries, concentric line). Estimation of heat transfer coefficients and pressure drops in two-phase rely on the correlation provided by Kandlikar (Kandlikar, 1990) and Friedel (Friedel, 1979), respectively. The estimated pressure drops in the detector at different operating pressures open to a double design approach, which is strongly dependent on the future operating range. Depending on the rated temperature (−70 or −80 °C), the system design and dynamic would change (Fig. 2). More specifically, if the lowest evaporating temperature is taken as reference and the flow under such conditions is maintained constant at different operating pressures, the vapor content at the exhaust two phase flow will increase under the same heat load and closer to the critical point (from 35 to 51 %). The drawback of such approach is the risk of dry-out at warmer temperatures. Vice versa, by taking the warmest temperature as reference would lead to an overflooded situation with an increase of the liquid content while progressing towards colder operation (quality falling from 35 to 24 %). The drawback is recirculating mainly liquid degrading the heat transfer, and the fluid would suffer by

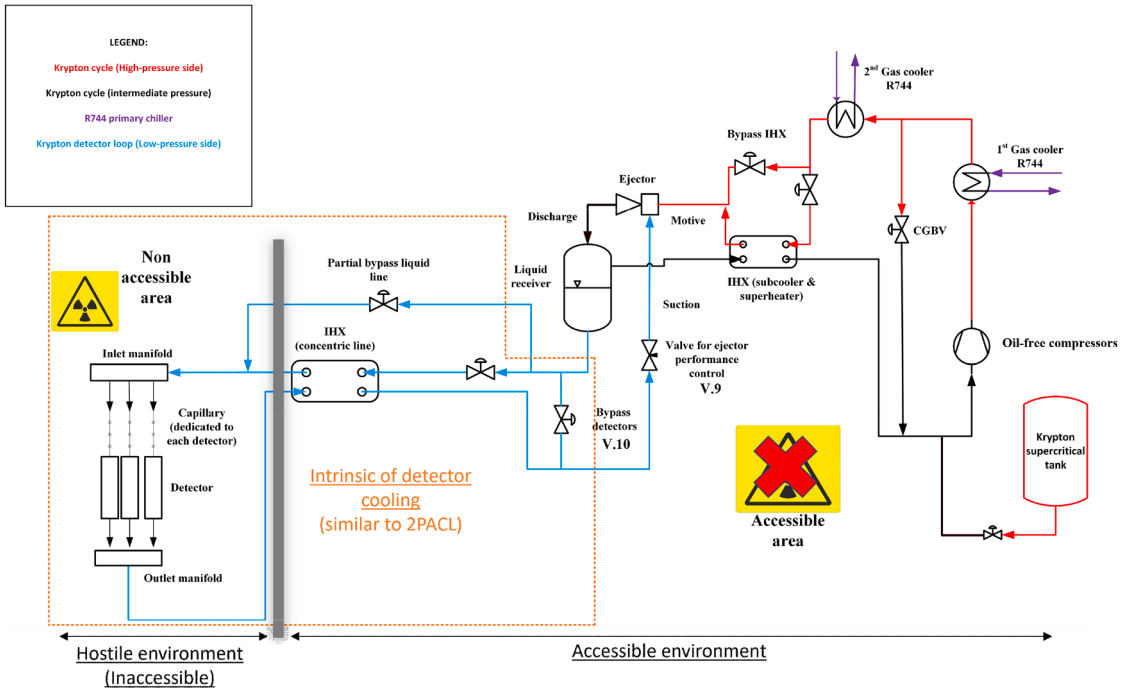

Fig. 1. Simplified architecture of the krypton cooling system.

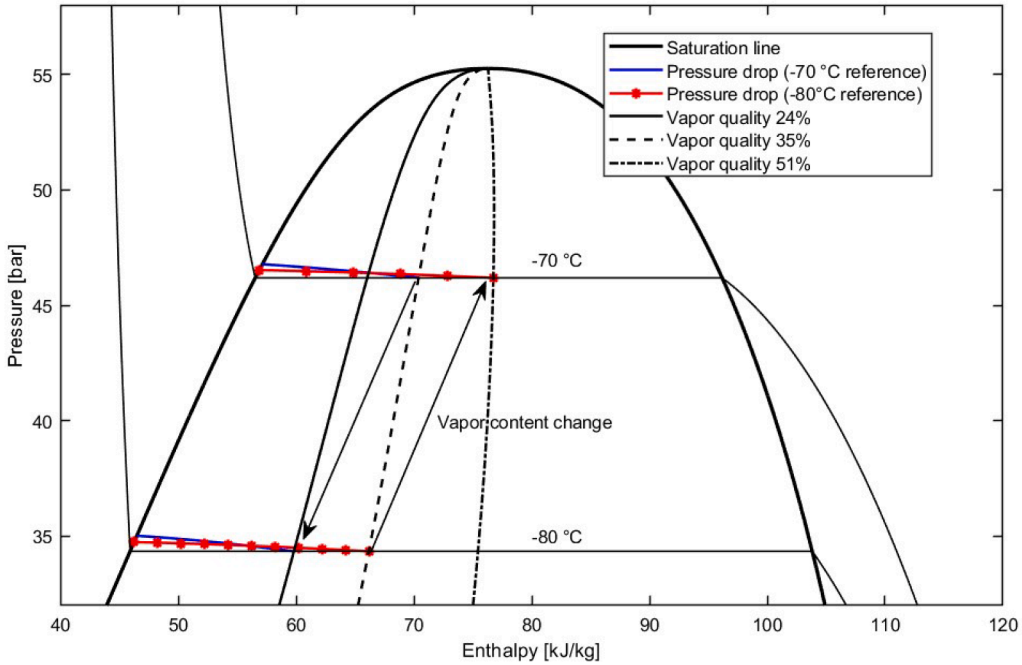

Fig. 2. Graphical representation in the p-h diagram of the implications deriving from the two proposed approaches.

larger temperature gradients at lower pressures. The highest evaporating temperature was chosen as reference to ensure the largest flow rate to make feasible the construction of a prototype controllable ejector, due to the limited cooling capacity of test unit.

The impossibility of actively regulating the flow through the evaporator channels and the floating heating powers from the experiments impose to introduce predominant pressure drops upstream the detector via the capillary such to suppress parallel boiling channel flow instabilities. Promoting a homogenous flow distribution is of critical importance such to ensure that, under the most unbalanced situation, the highest load in one of the cooling branches would still invoke enough flow to avoid dry-out. A predominant pressure drops upstream the evaporator in subcooled state is well known to be effective for hydraulic balancing of circuits with flowing medium.

The tube-in-tube heat exchanger must be sized considering the largest capacity which occurs at higher pressures where the enthalpy change is higher due to the compressibility of the liquid phase. The concentric line design is such that the subcooled liquid can potentially reach the outlet return temperature while ensuring as little pressure drops as possible in both feeding and return line. Except the small offset in the return two-phase line, controlling the ejector suction nozzle pressure allows a direct control of the evaporating temperature in the detector. The pressure lift, defined as the pressure difference between the liquid line at the bottom of the liquid receiver and the suction nozzle of the ejector (see Fig. 1), is maintained constant under all operating conditions.

The pumping capacity of the ejector strongly depends on the working conditions. It can refer to the ejector's ability to significantly increase the pressure of the secondary flow at the expense of the quantity of entrained refrigerant, or vice versa. The crossing points between the operational curve of the detector loop and the ejector defines the optimum geometry. The total cooling capacity of the demo system presented here, including three evaporators, is about 450 W, with a peak load in each cooling line up to 150 W. The cooling capacity applied in the study derives from the pixel modules installed in the innermost tracking layers, characterized by high volumetric power dissipation. In this area, the use of cold coolants as krypton is essential to maintain thermal stability after exposure to high radiation damage.

4. Dynamic modelling of the cycle

This section discusses the thermodynamic modelling of the system presented, with an overview of the modelling approach of the key components such as compressor and ejector. Additionally, a control strategy for transcritical operation of the system is proposed, aiming to maintain the thermal stability of the detector during typical transients encountered in physics experiments.

4.1. Model description

A dynamic model using Modelica object-oriented programming language in the Systemes, Dassault., 2022 environment was used to simulate the existing test setup built at the Varmeteknisk laboratory at NTNU (Trondheim, Norway). The physical-based model developed is based on the commercial library TIL-Suite HD 3.11 from TLK-Thermo GmbH (Richter, 2008) specifically developed for high-dynamic simulation with fast transients, using TIL-Media 3.11 library (Schulze, 2013) which consists of pre-loaded thermophysical properties of different pure fluids and mixtures. The only customized component was the tube-in-tube heat exchanger, since such geometry configuration was not included in the heat exchanger package offered in the library. Correlations previously mentioned for two-phase and single-phase flow (Darcy-Weisbach for pressure drops, Gnielinski for heat transfer) were implemented. A fuzzy modelling approach (Kim et al., 2021) was used to create a systematic interpolation through a weighted average of the different functions (correlations) that are valid only in their specific domain (single & two-phase state), providing a smooth transition when crossing the saturation line, aiming to avoid failure or stiffness for the solver. Despite the absence of krypton-rated components in the market, the authors opted for high-pressure rated components designed for CO_2, given their similarities with respect to operation envelope expressed in reduced pressure ($p_{crit,CO2}$= 73.77 [bar],$p_{crit,kr}$ = 55.25 [bar]). A small transcritical CO_2 Dorin compressor (model CD180H), with a swept volume of 1.12 m^3/h, was integrated into the prototype. While the use of an oil-lubricated compressor introduces challenges in terms of oil management, it is specific to the prototype and would not be a factor in the actual system. In the model, effects of oil were neglected. The reciprocating compressor was modelled following a physical-based

approach, where volume of suction and discharge chamber were considered in the dynamic energy and mass balances. For sake of simplicity the adjustable-needle ejector was modelled as an ejector with continuous modulation of the opening degree (reduction or increase of the throat of the motive nozzle) with a constant efficiency under all operating conditions (25 %), defined as in (Elbel, 2011). Because of the lack of studies on flashing of krypton, the motive flow rate was estimated using a built-in model for compressible flow (Brennen, 2005) offered in the TIL library.

4.2. Controlling strategies

Three main transient operation stages (startup, supercritical cool-down, and supercritical operation) precede the transcritical operation of the cycle. However, transition from supercritical to transcritical will be the subject of another study. Responding to variable load conditions in normal operation mode (transcritical cycle), the control logic should aim to:

- Ensure smooth and precise control of operational parameters, specifically flow rates and saturated temperature at the detector level. This typically occurs while the detectors are powered, due to the extensive electronics involved and the risk of electric failure from power cycling.
- Sizing the ejector to provide the primary and secondary stream mass flow rates requires five boundary conditions expressed in terms of pressure and density at the motive and suction port, as well as the outlet pressure. Maintaining one or more of these boundary conditions constant would simplify the ejector's sizing.

Although the cycle is more complex than a traditional low-pressure receiver cycle where an ejector is used for liquid recirculation, useful insights can be drawn from the transients triggered by either external (heat rejection medium) or internal variables (pressure). Specifically, if the gas cooler outlet temperature increases, warmer gas is expanded in the motive throat, causing a temporary rise of the receiver pressure. Conversely colder temperatures generate a rise of the liquid level and a drop of the receiver pressure. Similar effects occur via a reduction or enlargement of the annular flow passage in the throat. Any pressure fluctuations in the receiver will cause either colder or warmer krypton being carried over to the detectors. To respond to any perturbation in the system, the following logic was implemented:

- The high-pressure side is regulated and held to a fixed setpoint via the bypass valve downstream the first gas cooler (CGBV).
- The first gas cooler rejects the heat to the primary CO_2 chiller to control the outlet fluid temperature on the krypton side. This temperature is chosen such that expansion through the CGBV would always generate superheated vapor in case the IHX is not able to sustain an acceptable level of superheat.
- The receiver pressure is controlled via the heat rejection in the second gas cooler.
- The controllable ejector is modulated such to increase the entrainment potential, if required, by an increase of the motive stream flow rate at constant pressure. On the other hand, the entrainment potential is diminished by turning down the metering valve V.9 upstream the suction nozzle, as described in (Contiero et al., 2024), corresponding to the overfed scenario.

5. Results of the numerical study

In this section numerical results concerning the design of the semi-passive detector loop are first presented. The results obtained have been used as input in the dynamic model to assess the response of the system while applying the controlling strategies proposed in Section 4.2.

5.1. Steady-state performance analysis of the semi-passive detector loop

From the previous study (Contiero et al., 2024), geometry optimization of the cooling channel identified an inner tube diameter of 2 mm as most suitable for a 150 W detector cooling purposes, independently of the total cooling capacity of the system. Pressure drops and temperature gradients have been estimated first in the evaporator section which represents the core of the detector cooling loop. In two-phase state, as well as in single phase close to the critical point, thermophysical and transport properties change rapidly with pressure and density and therefore a finite difference method was used. Numerical evaluation was carried out in MATLAB (The MathWorks Inc. (2022)) where boundary conditions in terms of saturated liquid at the evaporator entrance, outlet quality and pressure are set. Fig. 3(a) shows the progressive increase in the flow required to maintain an outlet vapor quality of 35 % as it moves closer to the critical point due to the reduction of the latent heat. Fig. 3 (b) shows an example of pressure and fluid-wall temperature distribution along the cooling channel. The computed wall temperature profile is dependent on the correlation used, in which nucleate boiling and convective heat transfer coefficient are evaluated separately and their simultaneous contribution to the local heat transfer coefficient is not considered but rather the local maximum of them. The mass flow rate calculated at the highest evaporating temperature (−70 °C) was chosen as design flow.

Based on the estimated pressure drop in the evaporator section, the capillary was sized to introduce approximately a gradient four times higher than what observed in the evaporator. However, each capillary must be sized using experimental data as for small inner diameters the pressure drops are very sensitive to the inner rugosity of the pipe and to the uncertainty of the inner channel diameter. A tiny variation of the inner channel can lead to large uncertainty in the resulting pressure drop. An illustrative example is shown in Fig. 4.

As last, the concentric line was designed (Fig. 5): the feeding (liquid) line to the capillaries is placed on the inner side to be shielded from ambient heating, avoiding a double insulation due to the limited space. Liquid flow does not suffer higher pressure drops and pipes of reduced diameter can be used. The equivalent annulus diameter can be enlarged to reduce pressure losses in the return two-phase flow.

Close to the critical point, a non-linear variation of the specific heat capacity is registered leading to a non-linear variation of the liquid temperature along the feeding line. The extreme low temperature difference also implies an increase of the heat transfer area (length) as the heat flux drastically drops when the two stream's temperature approach each other. A minimum heat must be supplied to tune the inlet conditions to the detectors to low vapor quality to prevent from poor heat transfers (subcooled state). The minimum heat is obtained by bypassing part of the cold liquid to the mixing point upstream the capillary section. Therefore, by designing the line such as to potentially subcooled all liquid flow there will always be enough capacity (heat transfer area) under any operating conditions. Geometrical parameters of the detector loop are described in Table 1.

The semi-passive loop designed was simulated in Dymola environment to reach an overview of temperature, pressure and vapor mass fraction distribution as well as to verify the effectiveness of capillary pressure drops during possible unbalance of heating power in the different lines. The total ejector pressure lift estimated as sum of the pressure drops in the different components was around 3.2 bar. Fig. 6 shows pressure-temperature-quality profiles under the same setpoint in the detector (−70 °C) but under different heating powers (a-c, respectively).

The liquid temperature first decreases to approximately the same temperature at the outlet of the return line before being mixed at the capillary entrance. Across the capillary the main drop in pressure occurs, allowing low vapor quality flow (nearly saturated) to enter the evaporator. During nominal conditions where the three evaporators experience the same heat input (150 W), the vapor quality increases linearly

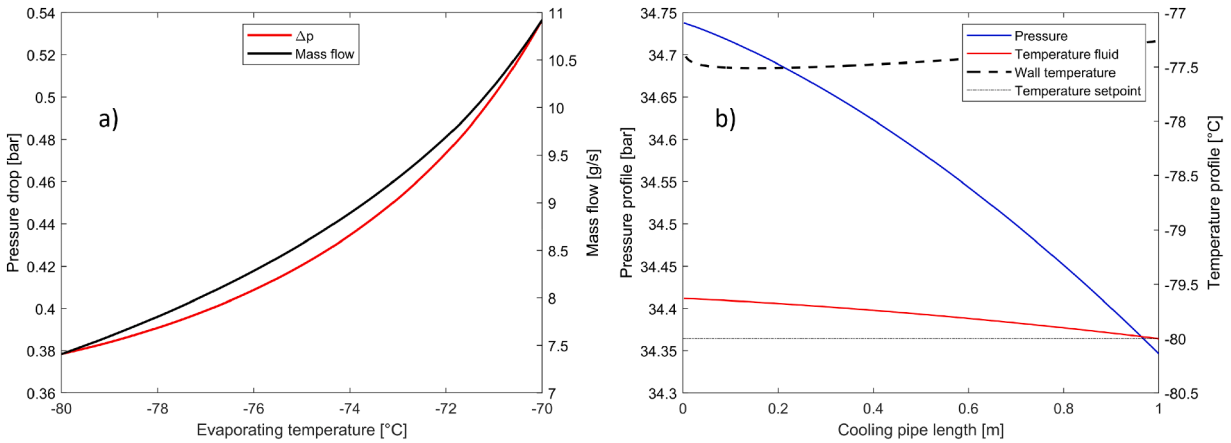

Fig. 3. Mass flow requirements and invoked corresponding pressure drop (a) for a standard detector (length= 1[m], d_i= 2 [mm] and heat load=150[W]) for reduced pressure in the range 0.62–0.84. Estimated pressure-temperature distribution along the cooling line (b).

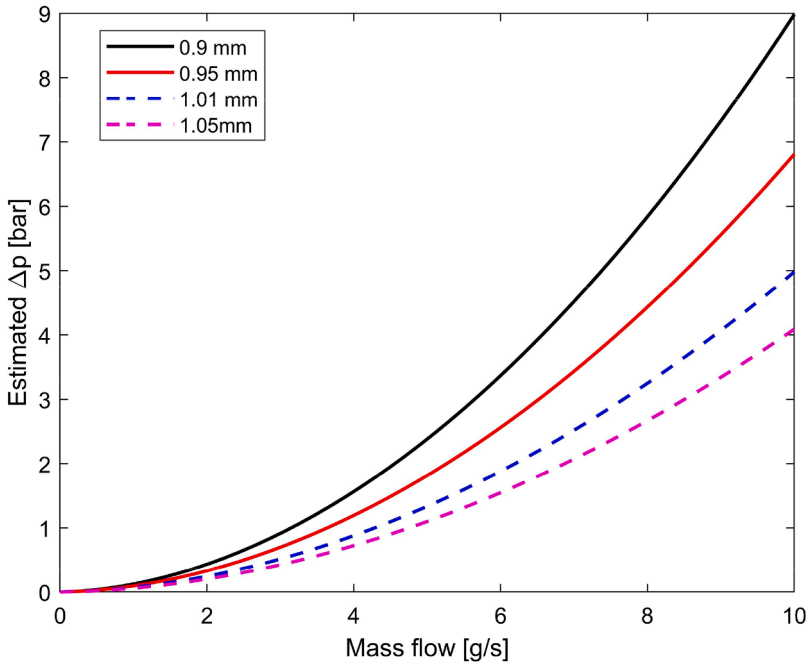

Fig. 4. Estimated pressure drops across a capillary for a given geometry (length = 0.5 m), under the same outlet conditions (subcooled state with $T = -80$ °C, $p = 48$ bars) but for different inner diameters.

up to 35 % due to the constant heat flux. Later the two-phase flow is further vaporized in the concentric line where initially the vapor quality has a slow increase. This zone corresponds to the area where the pinch point is registered.

The pressure drops across the unpowered line (in the capillary) is only slightly bigger than in the powered line (Fig. 6(c)). Predominant pressure drops in liquid state and the homogeneity of the two-phase flow at high working pressures help reducing the imbalance caused by fluctuating heating powers. At the manifold level, the powered line will almost receive the nominal flow as the difference compared to the unpowered line lies around 3 %. Due to the reference temperature of −70 °C and the constant pressure lift strategy, the liquid content increases as it progressively gets colder in the detector, regardless of the cooling power.

5.2. Transient performance of the cycle in various operational scenarios

The full-scale system was analyzed under the following dynamic scenarios, which are:

- A setpoint change starting from the highest allowed evaporating temperature (−70 °C) down to the lower limit (−80 °C).
- Arbitrary evaporating temperature (i.e. −70 °C) with an unbalance on the heating powers in the three different cooling lines.

Considering the different controllers implemented and interconnected, a preliminary study on expected fluid behavior in the detector loop (5.1) and required ejector working conditions (mainly in terms of pressure) need to be estimated to properly initialize the simulation model.

5.2.1. Floating setpoint

The first case concerns the variability of the working temperatures at the detectors: in any operating conditions it is essential to ensure an appropriate quantity of liquid such as to avoid the risk of dry-out and rapid thermal excursion. As the liquid content increases at the suction

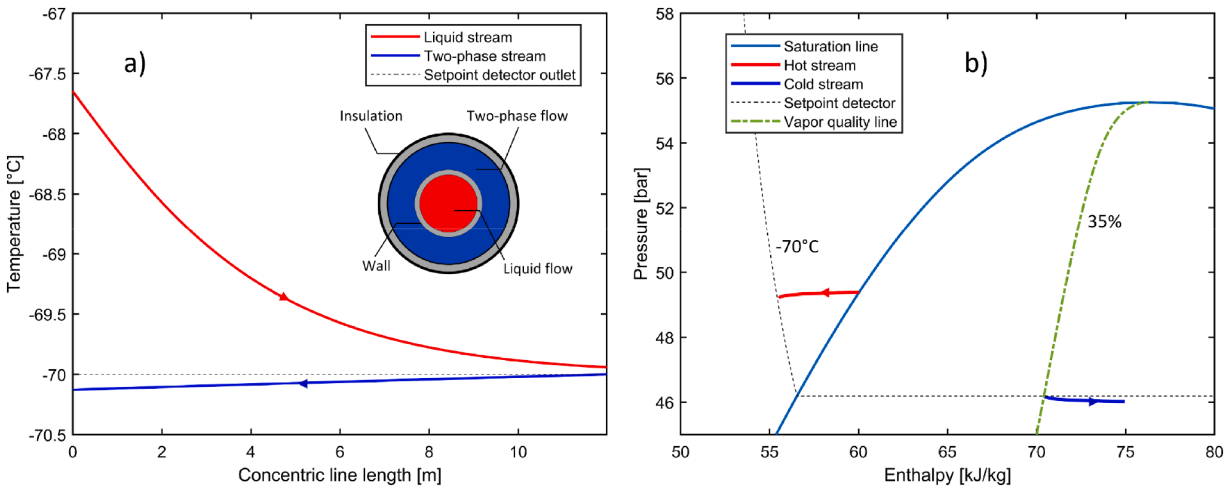

Fig. 5. Temperature profiles of the liquid & return two-phase flow (a). Representation in the p-h diagram (b).

Table 1
Geometry of the semi-passive loop designed for the test unit.

Concentric line	d_i [mm]	d_o [mm]	Thickness [mm]	Length [m]
Liquid line	6	8	1	12
Two-phase line	12	16	2	12
Capillary	1.01	1.59	0.29	0.14
Test section	2	2.4	0.2	1

nozzle port, the expansion work recovered per unit of flow increases due to the easier pre-compression of liquid compared to vapor. Since the ejector is modelled with constant efficiency, the valve V.9 is used to consume some part of the available expansion work, which increases as the receiver pressure is further reduced and pressure difference between the motive nozzle and ejector outlet increases. However, in practice a deterioration in ejector efficiency may be expected due to the increase of the liquid content under a constant motive flow, as the increase in density and viscosity leads to higher frictional losses and reduce the momentum exchange between primary and secondary flow. These

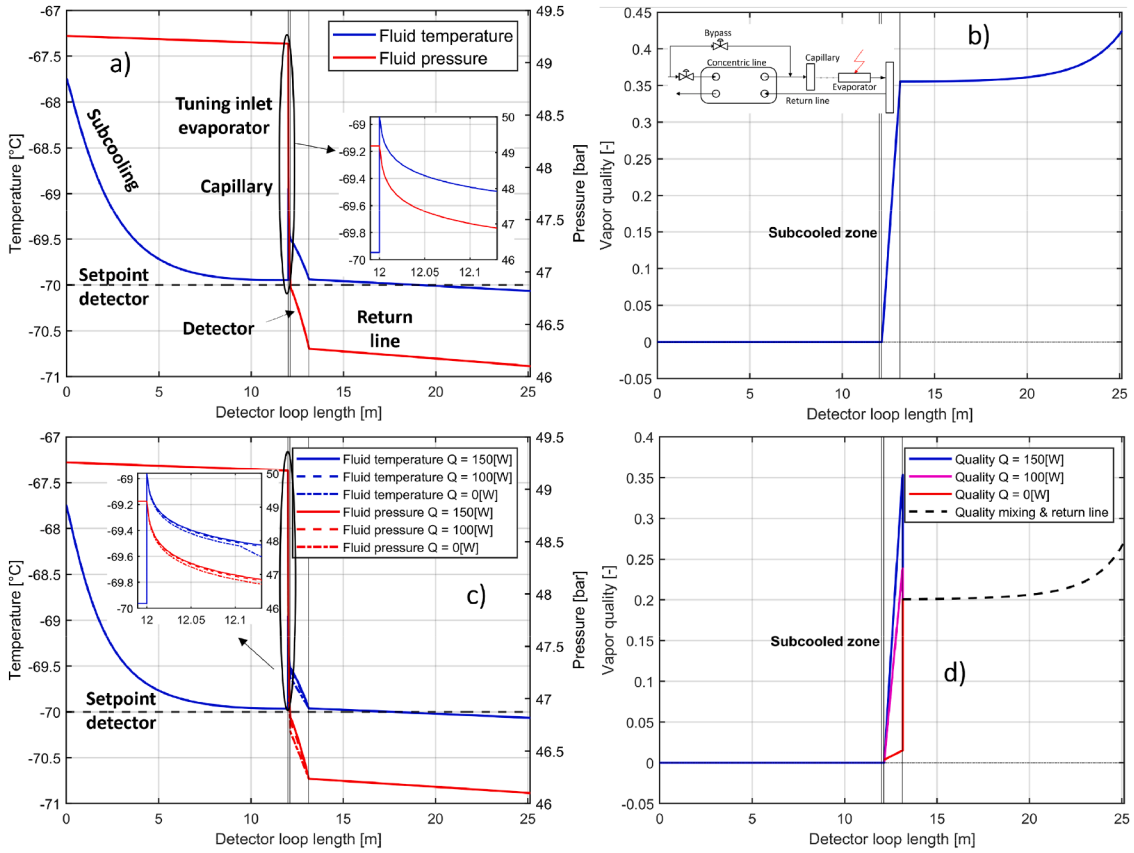

Fig. 6. Temperature, pressure and quality profiles along the detector loop (setpoint −70[°C], full load 450 [W]) (a,b). Same thermodynamic quantities with uneven heating load, i.e., different heating powers applied (150 W for evaporator 1100 W for evaporator 2 and 0 W for evaporator 3). Liquid line (0–12 m), capillary (12–12.14 m), evaporator (12.14–13.14 m), return line (13.14–25.14 m).

combined effects might require a different modulation of the pressure lift, or in case of a consistent drop of the ejector efficiency, a modulation of the nozzle throat area.

The gradual transition from the highest to the lowest setpoint is shown in Fig. 7. As the receiver pressure setpoint is lowered (b), the outlet temperature and vapor content in the detector decrease (c). Under constant motive pressure, larger expansion and warmer gas conditions, the ejector tends to boost the entrainment potential which is diminished using valve V.9 (d).

An assessment of the thermal load distribution relative to the heat load imposed on the detectors is shown in Table 2. Optimizing the compressor capacity would help in reducing the power consumption and the mass flow bypassed to the suction line through the bypass valve (CGBV). However, to allow the proposed cycle regulation, the compressor must remain oversized with respect to the ejector capacity.

5.2.2. Unbalanced thermal load on the detector

In this section, the stability of the system to sudden load changes is addressed. The same control logic can be applied here with the system responding as illustrated in Fig. 8. As one of the lines receives less power (c), vapor content at the detector outlet decreases (d). Under the same motive conditions, this corresponds to an increase in the entrained flow by the ejector (a), requiring valve V.9 to start closing (b). A slightly colder setpoint in the detector is reached due to the fixed fluid resistance in the loop. An additional advantage of operating at high reduced pressure is the limited change in the evaporating temperature as a function of the saturated pressure. As more lines start receiving less power, the great amount of liquid content causes a reduction in the opening degree of valve V.9 to maintain the total pressure drops across the detector loop nearly constant.

Table 3 illustrates the distribution of the heat loads in the system with different heating power in the detector, under a fixed evaporating temperature (−70 °C). At low heat loads, a great share of the compressor capacity is used by the ejector to produce a circulation of liquid krypton in the detectors to maintain them and the surrounding structure thermally cold, until the power from experiment is restored. This is of primary importance as a mechanical stress consequent the warming up of the support structure and the sensors could make some sections of the detector inoperative.

Table 2
Energy flow breakdown of the system with respect to the detector's heat load during floating setpoint.[11]

Temperature setpoint [°C]	Heat load [W]	Concentric line [%]	Compressor [%]	Gas cooler n° 1 [%]	Gas cooler n°2 [%]
−70 °C	450	19	202	189	113
−80 °C	450	11	250	296	54

6. Conclusion and future work

This work is part of a large study devoted to the development of a new cooling technology for particle detector cooling at CERN targeting temperatures below −50 °C. The ejector-supported cycle presented in the previous work served as starting point to derive design guidelines of the future full-scale system. The detectors, which represent the main heat source of the system, was used as starting point for a stepwise approach aimed at providing a cycle architecture that meets their strict requirements, such as spatial and temporal temperature gradient minimization, hardware compactness and remote control, essential due to the radioactivity level near the detectors.

The semi-passive detector loop was designed taking into account pressure losses, thermodynamic state of the fluid at the entrance of the detectors and hydraulic balance of multiple cooling lines via passive expansion devices. A relatively low vapor quality (35 %) at the detectors outlets was maintained in the initial design phase of the evaporative cooling lines. Since the power capacity per unit of flow varies at different temperatures (−70 to −80 °C), the design mass flow at −70 °C was used as reference to ensure spatial temperature stability at higher vapor pressures where the latent heat is reduced. However, studies on dry-out and boiling inception of krypton in minichannels will be required to verify whether boiling begins at the entrance of the pipe.

Capillary-based flow distribution system helps to trigger boiling at

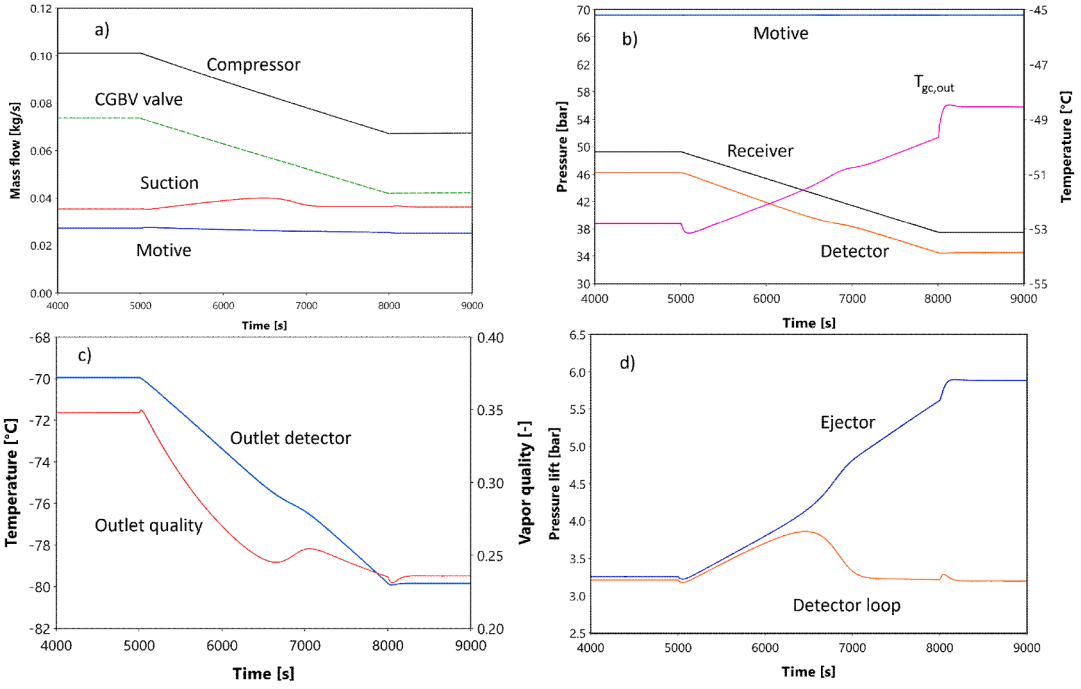

Fig. 7. Results from the dynamic transition of the detector's temperature, including mass flows (a), pressures and gas cooler outlet temperature(b), temperature and outlet quality at the detector level (c), as well as pressure lift seen by the ejector (d).

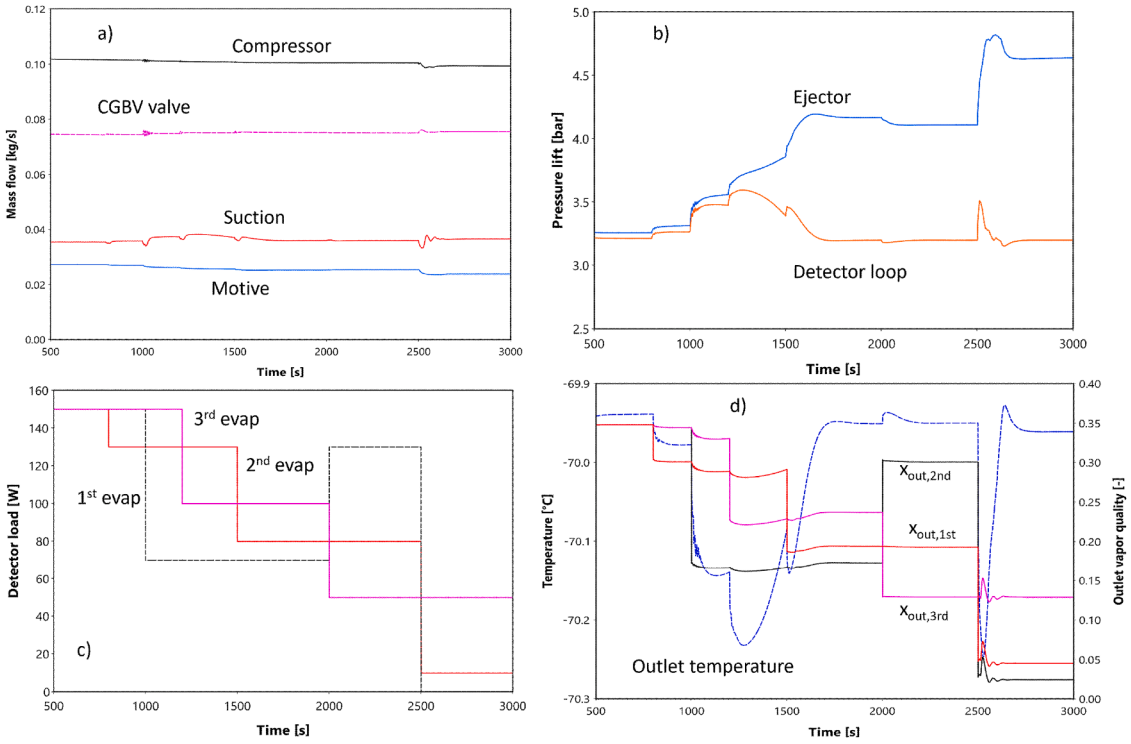

Fig. 8. System's response to a floating heating power from the experiments, including mass flows (a), pressure lift at the detector and ejector level (b), heating powers (c) and variation of the operating temperature and qualities at the outlet of the three sections (d).

Table 3
Energy flow breakdown during sudden change in the detector's heat loads.

Temperature setpoint [°C]	Heat load [W]	Concentric line [%]	Compressor [%]	Gas cooler n° 1 [%]	Gas cooler n°2 [%]
−70 °C	350	24	260	248	112
−70 °C	300	28	303	292	111
−70 °C	200	33	364	354	110
−70 °C	60	615	1484	1514	70

the entrance of the detector and to minimize a detector loop failure. Pressure drops introduced by the capillary are approximately four times higher than the evaporator pressure drops. Numerical assessments confirm that near the critical point an even flow distribution in each detector cooling line can be achieved, maintaining the design mass flow rate independently of the unbalance of the heat load. The pressure upstream of the capillary defines the heat load exchanged in the counter-flow tube-in-tube heat exchanger, which was designed to introduce a small offset in pressure (below 0.2 bar) in the return line to enable a direct control of the evaporating temperature via the ejector. A total pressure lift of the ejector equal to the overall pressure drop in the detector loop, was estimated to be approximately 3.2 bar. In the optics of simplifying the system control, a constant ejector pressure lift strategy was adopted. However, this approach may entail potential disadvantages such as a reduced heat transfer coefficient at lower evaporating temperatures, resulting from a decreased vapor mass fraction, according to typical flow pattern profiles in flow boiling. Within the investigated range of the high reduced pressure in the evaporator where the overall pressure drops might be attributed to liquid and gas phase approximately in the same proportion, the main drop in pressure constantly occurs along the capillary line. Consequently, flow variation does not exceed 4.3 % of the design value while operating at −80 °C.

A dynamic model was built in Dymola and supported by a control logic to numerically assess what would be the response of the system to a setpoint change or floating heat loads. The receiver pressure setpoint is relevant as it is closely associated with the operating temperature in the detectors. The heat rejection in the gas cooler section controls the receiver pressure, acting against a sudden change in pressure in the tank consequent to a setpoint or heat load change. Increasing the ejector pressure lift via valve V.9 serves to modulate the flow whenever the detector is overfed. During the gradual setpoint change towards −80 °C, the pressure lift seen by the ejector moves from 3.2 bars to 5.9 bars in order to reduce the excessive entrained flow, under the assumption of constant ejector efficiency. Nevertheless, if the ejector efficiency drops, the ejector pressure lift will be reduced so requiring a different modulation of valve V.9. In the event of a significant efficiency drop that compromises the secondary flow through the detector, modulation of the motive pressure will be necessary to boost the pumping capacity. Therefore, if a constant-efficiency-based-model will prove to be unsatisfactory, modulation of the needle will be required to supply the desired flow conditions. In case of fluctuating heat loads from the detector electronics, resembling the scenario of an electrical fault of the sensors, modulation of valve V.9 will limit the thermal excursion of the evaporating temperature to below 0.3 K, under the assumption of constant ejector efficiency as described above. An assessment of the energy flow profile, both under a setpoint change and unbalanced heat loads from the detector electronics, shows that the energy flow introduced by the compressor is much larger than the cooling load. This is a consequence of: the availability of high-pressure rated reciprocating compressors in the market with a limited swept volume, the assumed ejector efficiency in the model, the limited cooling capacity of the refrigeration system presented.

Future work will first focus on developing a control logic for transient operational periods of specific importance, as startup and

[1] The values of the energy profiles are calculated based on the assumption of the ejector efficiency (25%), as the inlet motive pressure has a direct impact on the compression power.

cooldown, based on the cycle designed in the current work. Secondly, heat transfer and pressure drop measurements in minichannels must be conducted to validate and refine the numerical design tool. A test campaign on the compressor performance must be conducted to evaluate the available cooling capacity relative to the demand from the ejector, ensuring it meets the flow requirements of the detectors. Additionally, a detailed performance map of the two-phase ejector, along with the impact of vapor inlet quality at the suction nozzle on the ejector performance, must be thoroughly examined before launching the experimental campaign.

Nomenclature

Symbols	
d	diameter (mm)
x	Vapor quality (-)
T	Temperature (K, °C)
Subscripts	
i	Inner
o	Outer
gc,out	Gas cooler outlet
out,1st	Outlet first evaporator
out,2nd	Outlet second evaporator
out,3rd	Outlet third evaporator
kr	Krypton
Acronyms	
CGBV	Cold gas bypass valve
IHX	Internal heat exchanger
Δp	Pressure drop (bar)

CRediT authorship contribution statement

Luca Contiero: Writing – original draft, Visualization, Software, Methodology, Investigation, Conceptualization. **Krzysztof Banasiak:** Writing – review & editing, Supervision, Conceptualization. **Bart Verlaat:** Supervision, Resources, Project administration, Conceptualization. **Armin Hafner:** Supervision, Resources, Project administration, Funding acquisition. **Sven Försterling:** Writing – review & editing, Supervision, Software. **Yosr Allouche:** Writing – review & editing, Supervision, Project administration.

Declaration of competing interest

The authors declare that they have no known competing financial interests or personal relationships that could have appeared to influence the work reported in this paper.

Acknowledgements

This research work is supported by the European Union's Horizon 2020 research and innovation program, 'AIDAInnova project' (grant number 101004761).

References

Anderssen, E., 1999. Fluorocarbon evaporative cooling developments for the ATLAS pixel and semiconductor tracking detectors. in. In: 5th Workshop on Electronics for the LHC Experiments (LEB 99, pp. 421–426.

ATLAS collaboration, 1997. ATLAS Inner Detector: Technical Design Report - Vol I. CERN.

Attree, D., 2008. The evaporative cooling system for the ATLAS inner detector. J. Inst 3, P07003. https://doi.org/10.1088/1748-0221/3/07/P07003.

Attree, D., Anderson, B., Anderssen, E.C., Akhnazarov, V., Apsimon, R.J., Barclay, P., Batchelor, L.E., Bates, R.L., Battistin, M., Bendotti, J., Berry, S., Bitadze, A., Bizzel, J. P., Bonneau, P., Bosteels, M., Butterworth, J.M., Butterworth, S., Carter, A.A., Carter, J.R., Catinaccio, A., Corbaz, F., Danielsson, H.O., Danilevich, E., Dixon, N., Dixon, S.D., Doherty, F., Dorholt, O., Doubrava, M., Egorov, K., Einsweiler, K., Falou, A.C., Feraudet, P., Ferrari, P., Fowler, K., Fraser, J.T., French, R.S., Galuska, M., Gannaway, F., Gariano, G., Gibson, M.D., Gilchriese, M., Giugni, D., Godlewski, J., Gousakov, I., Gorski, B., Hallewell, G.D., Hartman, N., Hawkings, R.J., Haywood, S.J., Hessey, N.P., Ilyashenko, I., Infante, S., Jackson, J.N., Jones, T.J., Kaplon, J., Katunin, S., Lindsay, S., Luisa, L., Massol, N., McEwan, F., McMahon, S.J., Menot, C., Mistry, J., Morris, J., Muskett, D.M., Nagai, K., Nichols, A., Nicholson, R., Nickerson, R.B., Nielsen, S.L., Nordahl, P.E., Olcese, M., Parodi, M., Perez-Gomez, F., Pernegger, H., Perrin, E., Rossi, L.P., Rovani, A., Ruscino, E., Sandaker, H., Smith, A., Sopko, V., Stapnes, S., Stodulski, M., Tarrant, J., Thadome, J., Tovey, D., Turala, M., Tyndel, M., Vacek, V., van der, Kraaij E., Viehhauser, G.H.A., Vigeolas, E., Wells, P. S., Wenig, S., Werneke, P., 2008. The evaporative cooling system for the ATLAS inner detector. J. Instrum. 3, P07003. https://doi.org/10.1088/1748-0221/3/07/P07003.

Battistin, M., Berry, S., Bitadze, A., Bonneau, P., Botelho-Direito, J., Boyd, G., Corbaz, F., Crespo-Lopez, O., Riva, E.D., Degeorge, C., Deterre, C., DiGirolamo, B., Doubek, M., Favre, G., Godlewski, J., Hallewell, G., Katunin, S., Lefils, D., Lombard, D., McMahon, S., Nagai, K., Robinson, D., Rossi, C., Rozanov, A., Vacek, V., Zwalinski, L., 2015. The thermosiphon cooling system of the ATLAS experiment at the CERN large hadron collider. Int. J. Chem. React. Eng. 13, 511–521. https://doi.org/10.1515/ijcre-2015-0022.

Beck, G., Viehhauser, G., 2010. Analytic model of thermal runaway in silicon detectors. Nucl. Instrum. Methods Phys. Res. A 618, 131–138. https://doi.org/10.1016/j.nima.2010.02.264.

Brennen, C.E., 2005. Fundamentals of Multiphase Flow. Cambridge University Press, Cambridge. https://doi.org/10.1017/CBO9780511807169.

Contiero, L., Verlaat, B., Hafner, A., Banasiak, K., Allouche, Y., Petagna, P., 2024. A new cold cooling system using krypton for the future upgrade of the LHC after the long shutdown 4 (LS4). Nucl. Instrum. Methods Phys. Res. A 1064, 169420. https://doi.org/10.1016/j.nima.2024.169420.

ECFA Detector R&D Roadmap Process Group, 2020. The 2021 ECFA detector research and development roadmap. https://doi.org/10.17181/CERN.XDPL.W2EX.

Elbel, S., 2011. Historical and present developments of ejector refrigeration systems with emphasis on transcritical carbon dioxide air-conditioning applications. Int. J. Refrig. Eject. Technol. 34, 1545–1561. https://doi.org/10.1016/j.ijrefrig.2010.11.011.

Friedel, L., 1979. Improved friction pressure drop correlations for horizontal and vertical two-phase pipe flow. In: European Two-Phase Group Meeting. Ispra, Italy.

Kandlikar, S.G., 1990. A general correlation for saturated two-phase flow boiling heat transfer inside horizontal and vertical tubes. J. Heat Transf. 112, 219–228. https://doi.org/10.1115/1.2910348.

Kim, D., Ma, J., Braun, J.E., Groll, E.A., 2021. Fuzzy modeling approach for transient vapor compression and expansion cycle simulation. Int. J. Refrig. 121, 114–125. https://doi.org/10.1016/j.ijrefrig.2020.10.025.

Mahapatra, P., 2018. Advanced regulatory control of a 10 MWe supercritical CO2 recompression brayton cycle towards improving power ramp rates.

Moisseytsev, A., Kulesza, K.P., Sienicki, J.J., 2009. Control System Options and Strategies For Supercritical CO2 cycles. (No. ANL-GENIV-081). Argonne National Lab. (ANL),, Argonne, ILUnited States. https://doi.org/10.2172/958037.

Pettersson, T.S., Lefèvre, P. (Eds.), 1995. Large Hadron Collid..

Richter, C., 2008. Proposal of new object-oriented equation-based model libraries for thermodynamic systems. https://doi.org/10.24355/dbbs.084-200806100200-3.

Schulze, C.W., 2013. A Contribution to Numerically Efficient Modelling of Thermodynamic Systems. dissertation. Technical University Braunschweig, Braunschweig Germany.

Seidel, S., 2019. Silicon strip and pixel detectors for particle physics experiments. Phys. Rep. 828, 1–34. https://doi.org/10.1016/j.physrep.2019.09.003.

Systemes, Dassault., 2022. DYMOLA Systems Engineering. Multi-Engineering Modeling and Simulation based on Modelica and FMI. https://scholar.google.com/scholar?q=Dassault%20Systems%2C%20DYMOLA%20Systems%20Engineering%3A%20Multi-Engineering%20Modeling%20and%20Simulation%20based%20on%20Modelica%20and%20FMI%2C%202022.%20Available%20from%3A%20%3Chttps%3A%2F%2Fwww.3ds.com%2Fproducts-services%2Fcatia%2Fproducts%2Fdymola%2F%3E.

The MathWorks Inc. (2022), Natick, Massachusetts: The MathWorks Inc. MATLAB version: 9.12.0 (R2022a).

Trinh, T., 2010. Dynamic response of the supercritical CO 2 brayton recompression cycle to various system transients.

Tropea, P., Daguin, J., Petagna, P., Postema, H., Verlaat, B., Zwalinski, L., 2016. CO2 evaporative cooling: the future for tracking detector thermal management. Nucl. Instrum. Methods Phys. Res. A 824, 473–475. https://doi.org/10.1016/j.nima.2015.08.052. Frontier Detectors for Frontier Physics: Proceedings of the 13th Pisa Meeting on Advanced Detectors.

Van Es, J., Van Donk, G., Pauw, A., Rens, C., Jaarsma, J., Brouwer, M., Verlaat, B., 2004. SAE Technical Paper.

Verlaat, B., 2007. Controlling a 2-phase CO 2 loop using a 2-phase accumulator.

Verlaat, B., Lysebetten, A., van Beuzekom, M., 2008. CO2 cooling for the LHCb-VELO experiment at CERN. In: Proceedings on the 8th IIF/IIR Gustav Lorentzen Conference on Natural Working Fluids. Presented at the Proceedings on the 8th IIF/IIR Gustav Lorentzen Conference on Natural Working Fluids. Copenaghen.

Zhang, Z., Sun, X.-H., Tong, G.-N., Huang, Z.-C., He, Z.-H., Pauw, A., van Es, J., Battiston, R., Borsini, S., Laudi, E., Verlaat, B., Gargiulo, C., 2011. Stable and self-adaptive performance of mechanically pumped CO2 two-phase loops for AMS-02 tracker thermal control in vacuum. Appl. Therm. Eng. 31, 3783–3791. https://doi.org/10.1016/j.applthermaleng.2011.07.015.

Zwalinski, L., Barroca, P., Bortolin, C., Bhanot, V., Collot, J., Daguin, J., Davoine, L., Doubek, M., Giakoumi, D., Hanf, P., Herpin, Y., Hulek, W., Noite, J., Pakulski, T., Petagna, P., Sliwa, K., Verlaat, B., 2023. Progress in new environmental friendly low temperature detector cooling systems development for the ATLAS and CMS experiments. Nucl. Instrum. Methods Phys. Res. A 1047, 167688. https://doi.org/10.1016/j.nima.2022.167688.